Quantitative site-level information on the potential carbon sink saturation effect

using data from Work Package 2, Task 2.1

CLIMB-FOREST

Deliverable title:	Quantitative site-level information on the potential carbon sink saturation effect in Task 2.1
Author:	Holger Lange (NIBIO), Natalia Kowalska (GCB)
Citation:	Reference
Deliverable number:	2.2
Work package:	2 (Task 2.1)
Lead partner:	GCB
Due date of deliverable:	30.09.2025
Submission date:	11.03.2026
Dissemination Level	Public
Reviewed by	

Version	Date	Modified by	Modification reasons
D1	Date	Name	e.g. Add changes from review

The sole responsibility for the content of this publication lies with the authors. It does not necessarily represent the opinion of the European Commission, which is not responsible for any use that may be made of the information contained therein.

Contents

List of Figures

D2.2 Quantitative site-level information on the potential carbon sink saturation in Task 2.1

1. Introduction

Anthropogenic Greenhouse Gas (GHG) emissions are rising, and the concentration of CO_2 as the most important GHG is increasing in the atmosphere accordingly. However, part of the emissions added through human activity are absorbed again by our ecosystems, both in the oceans and on land. The amount of CO_2 taken up again is estimated to be around 50% of our emissions (20.4 $GtCO_2$ yr^{-1} for the 10-year period 2015-2024, with a budget imbalance smaller than 1%), but the relative contribution of ocean and land ecosystems is rapidly changing – less and less is taken up by the land ecosystems, the newest number being 21% of all emissions, or 8.7 $GtCO_2$ yr^{-1} (Friedlingstein et al., 2025). The land sink is rapidly weakening.

There are numerous explanations around for this phenomenon, including biased calculations of the Global Carbon Budget in the past (Randerson et al., 2025), but there is strong evidence that the forest sink is rapidly decreasing during most recent years (Korosuo et al., 2023).

Rising CO_2 concentrations in the atmosphere might be expected to be beneficial for plant productivity, since they might photosynthesize more with the same amount of transpiration losses, or conversely reduce transpiration loss at the same level of carbon fixation (increased intrinsic Water Use Efficiency). Water Use efficiency (WUE) is a measure of the amount of carbon a plant can fix per unit of water lost through transpiration. In many studies, an increase in atmospheric CO_2 is thought to enhance WUE, potentially boosting plant growth under certain conditions. On the other hand, there might be adaptation processes like reduced stomata opening, leading to a diminishing of productivity over time, as amply demonstrated through a series of FACE experiments (Norby and Zak, 2011). (FACE – Free-Air CO_2 Enrichment experiments have been crucial in studying the effects of elevated CO2 on plant productivity in natural settings, providing long-term data on forest responses.)

It has been long suggested that the forest sink might eventually saturate with ever higher atmospheric CO_2 concentrations (Nabuurs et al., 2013; Nabuurs et al., 2003). Phenotypic plasticity, increased likelihood of stressors, or fundamental metabolic processes might prevent trees from utilizing additional CO_2 with the same efficiency. The empirical evidence for this “sink saturation hypothesis” is so far mostly either based on remote sensing products (Wang et al., 2020) or utilizes the outputs from Terrestrial Biome Models (Shi et al., 2021).

WP2 of CLIMB-FOREST makes extensive use of site-level measurements from flux tower locations. Flux towers measure the exchange of relevant gases (e.g. CO_2 or H_2O) between the ecosystem and the atmosphere providing valuable data for carbon fluxes and allowing us to track the strength and direction of the forest sink over time. Some of them have a sufficiently long record to investigate whether there are signs of a sink saturation for carbon uptake in forests.

The next chapter describes our approach to quantify the trend in sink strength, based on CO_2 concentrations and ecosystem-scale carbon fluxes. This approach will allow us to assess whether forest ecosystems are showing signs of diminished carbon uptake in response to rising atmospheric CO_2 levels. The sites selected for this analysis are listed in the next chapter, followed by the results for the sink strength at the individual sites

as well as for the whole dataset combined. We conclude on the sink saturation hypothesis in the final chapter where we summarize our findings, discuss potential mechanisms behind these trends and consider the implications for future carbon budget projections.

2. How to quantify carbon uptake efficiency

At all sites with Eddy Covariance (EC) equipment, the carbon flux Net Ecosystem Exchange (NEE) or Net Ecosystem Productivity (NEP) is directly observed at footprint level. From that, using a small set of standardized procedures and assumptions, the ecosystem-level transpiration losses and thus the Gross Primary Productivity (GPP) are estimated. We base the identification of a possible trend in carbon uptake on these two fluxes, NEE and GPP.

Due to the presence of an Infrared Gas Analyzer at each EC site, local atmospheric CO2 concentrations are also available as time series with high temporal resolution. We consider that CO2 concentration as driving variable, and either NEE and GPP as response. Of course, the two carbon fluxes are also determined by many other factors, but for the potential carbon sink saturation, which is the diminishing response of ecosystem carbon uptake to increasing concentrations, this simple concept serves the purpose.

There are several methods published for the quantification of the connection between carbon concentration and flux. They have in common that they operate on long time scales of at least several years. Annual or even seasonal carbon fluxes are highly variable and impacted by peculiar weather conditions, extreme events, and disturbances. These short-term episodes are irrelevant to the hypothesis to be checked. However, a major disturbance which is stand-replacing, be it natural (fire, windthrow, pathogens) or management-induce (clearcuts or other major silvicultural operations) disqualifies the dataset for further investigation, as the young stand emerging at the site after the event follows a rather different carbon uptake trajectory in the first years, typically being a source rather than a sink initially.

In order that possible trends in the carbon flux and CO_2 concentrations might not be masked by high interannual variability, the notorious seasonal scale, and disturbances, we work with annual means only, consider a feasible time lag (a couple of years) which is, however, a parameter not set to a fixed value, and a number of different sites since we are interested in average behaviour, not the peculiarities of one particular site. Assuming that there is a power-law connection between yearly average GPP and CO_2 concentrations:

$$GPP(t) = c \cdot CO_2(t)^{\beta} \quad (1)$$

where c is a “constant” with a complicated unit depending on the value of β, but is also site-specific and integrates climate, plant functional type, management, and other aspects of the forest in question, we see that $\beta = 1$ indicates a linear relationship, $\beta = 0$ would mean that gross productivity is independent from CO_2 levels, and the unexpected $\beta < 0$ implies that production diminishes with increasing CO_2. A declining relative benefit from additional atmospheric carbon is observed when $0 < \beta < 1$.

We are interested in temporal trends in β and thus compare its estimates over long periods of time. Taking ratios from eq. (1) at two different moments in time

$$\frac{GPP(t+\Delta t)}{GPP(t)} = \left(\frac{CO_2(t+\Delta t}{CO_2(t)}\right)^{\beta(t)} \quad (2)$$

where Δt is a time lag (a number of years) which is a parameter of the method, we get rid of the "constant" c from eq. (1) and are able to extract an estimate for $\beta(t)$:

$$\beta(t) = \frac{log\left(\frac{GPP(t+\Delta t}{GPP(t)}\right)}{log\left(\frac{CO_2(t+\Delta t}{CO_2(t)}\right)} \quad (3)$$

This is the method to determine β which is also used by (Walker et al., 2021). Note that it refers to a relation between carbon flux and concentration, where time is only implicit. We still consider a time-dependent $\beta(t)$ and thus its temporal trends since we expect monotonously increasing annual CO_2 concentrations as a function of time, the hallmark of climate change. However, this might not be the case for some of the sites with rather peculiar conditions, as will be elucidated in the next chapter.

When replacing GPP with NEE, there might be cases where the system was a net sink in one of the two years and a source in the other. The sign of the annual NEE is different in that case, rendering the logarithm in eq. (3) imaginary. These situations have to be excluded and indicate also that NEE is a less robust carbon flux to use for checking the sink saturation hypothesis.

After calculating $\beta(t)$ values for all sites and values for relevant time lags Δt, we will perform a trend analysis (a simple least-squares regression) to determine whether the carbon sink saturation hypothesis, indicated through significant negative temporal trends, can be confirmed through this analysis. That would be the case if a majority of the sites, or alternatively the mean $\beta(t)$ over all sites, shows a significant negative trend.

3. Selection of suitable sites

Length requirements

The slope calculations require long records of annual GPP and NEE measurements. Furthermore, a meaningful minimum number of sliding windows of length Δt must be obtainable to allow the calculation of the trend in $\beta(t)$. The relevant window lengths are 5 years or longer; we decided to require at least **10 years** of consecutive annual values for GPP and NEE. This restriction led to the selection of 22 sites from 9 countries. An overview of some of their properties is provided in Table 1. Among these, there are some "classical" ecosystem stations installed as Eddy Covariance sites long before ICOS was started in 2015. These sites have been, and are still, part of Fluxnet or Ameriflux. The sites span a large range of species composition, stand age, climate, elevation, and different type of management regimes are also present. They have the potential to be representative of European and North American forests; if there are systematic carbon sink

saturation effects, they should show up in these stands. The broad geographic and ecological coverage of these sites makes them suitable for detecting potential trends in carbon sink saturation across different forest types and climate conditions.

Local versus global CO_2 concentrations

Every flux tower site measures CO_2 concentrations (usually at high frequencies, like 20 Hz) locally through the installed Infrared Gas Analyzers (IrGAs). The concentration time series, combined with 3D wind measurements, serve as fundamental inputs for the flux calculations. However, IrGAs need recalibration, may malfunction, and might not properly represent the local concentration very well. Whereas concentrations at higher temporal resolution (e.g. daily or sub-daily) reflect the local uptake and emission within the tower footprint, CO_2 is a gas that is very well-mixed in the global atmosphere, with equilibration periods of weeks to months within the same hemisphere. Thus, annual CO_2 concentrations might as well be represented by global products which are unbiased, quality-controlled and gap-free. In this report, we use the monthly mean global CO_2 time series from the Global Monitoring Lab[1] which is available from 1980 onwards. Results will be based on both the local as well as the global concentration data. This dual approach allows for a more robust comparison and evaluation of flux tower data in the context of broader atmospheric trends.

[1] https://gml.noaa.gov/ccgg/trends/global.html#global

Table 1: The sites used to estimate β values. Acronyms are: BE: Belgium; CH: Switzerland; DE: Germany; FI: Finland; FR: France; IT: Italy; NL: The Netherlands; US: United States of America; masl: meter above sea level; ENF: Evergreen Needle Forest; MF: Mixed Forest; DBF: Deciduous Broadleaf Forest; WET: Wetland Forest; WSAV: Woody Savanna; H: Mean tree height; CCF: Continuous Cover Forestry. Table elements where the entry is not known to us are left blank.

Site Name	Acronym	Latitude	Longitude	Elevation (masl)	Forest type	Age in 2026 (years)	H (m)	Management	EC years
Brasschaat	BE-Bra	51.30761	4.51984	24	ENF	99	11	Unknown	1996-2023
Vielsalm	BE-Vie	50.304962	5.998099	497	MF	103	18	Unknown	1996-2023
Davos	CH-Dav	46.81533	9.85591	1660	ENF	256	17	CCF	1997-2023
Laegern	CH-Lae	47.478333	8.364389	706	MF			CCF	2004-2021
Stitna	CZ-Stn	49.035975	17.9699	562	DBF	124	32	Clear-Cut	2010–2020
Hainich	DE-Hai	51.07921	10.45217	470	DBF	143	35	Unmanaged	2000-2022
Hetzdorf	DE-Hzd	50.963806	13.489778	390	DBF	33		CCF	2010-2023
Leinefelde	DE-Lnf	51,3282167	10.3678	489	DBF	138	35	Unknown	2002-2012
Hyytiälä	FI-Hyy	61.84741	24.29477	183	ENF	65	21	Clear-Cut	1996-2023
Lettosuo	FI-Let	60.64183	23.95952	128	ENF	53	14	CCF	2009-2020

Fontainebleau-Barbeau	FR-Fon	48.476357	2.780096	117	DBF	153	15	CCF	2005-2023
Le Bray	FR-LBr	44.7171	-0.7693	62	ENF	58	20	Unknown	1996-2008
Collelongo	IT-Col	41.8494	13.5881	1543	DBF	137	22	CCF	1996-2014
Castelporziano	IT-Cpz	41.7052	12.3761	23	EBF			Unknown	1997-2009
Lavarone	IT-Lav	45.9562	11.28132	1353	ENF	111	28	Unknown	2003-2014
Renon first dataset	IT-Ren1	46.58686	11.43369	1739	ENF	128		Unknown	1998-2023
Renon second dataset	IT-Ren2	46.58686	11.43369	1739	ENF	128		Unknown	1999-2023
Loobos	NL-Loo	52.166447222	5.74355	34	ENF	118	17	Unknown	1996-2023
Harvard Forest	US-Har	42.5378	-72.1715	344				Unmanaged	1991-2024
Mt. Bigelow	US-MtB	32.416	-110.7256	2593	ENF			Thinned	2009-2021
Alligator River	US-NC4	35.7879	-75.9038	0	WET			Protected	2009-2024
Tonzi Ranch	US-Ton	38.4309	-120.966	171	WSAV			Unmanaged	2001-2024

4. Results for the carbon uptake slopes

Dependence on the time window length

The slopes $\beta(t)$ as calculated according to eq. (3) could as well have an index Δt since there is an obvious dependence on the chosen time window length. This dependence will be studied in more detail now.

To cope with substantial interannual variability, the shortest time window length considered as meaningful is set to 5 years. The choice for the longest time window is constrained by the temporal coverage of the site data. We chose a maximum of 12 years, an upper bound which is already excluding some of the sites from the analysis.

Using site-specific concentrations, some of the $\beta(t)$ values can get unreasonably high magnitude. The most frequent reason is very small differences in local annual CO_2 concentrations, leading to a very small denominator of eq. (3) and thus blowing up β. In some cases, one of the two years either at the beginning or at the end of the respective windows has been extreme in terms of NEE or GPP, implying a potentially large magnitude of the numerator as well. For the trend analysis, these outliers are discarded.

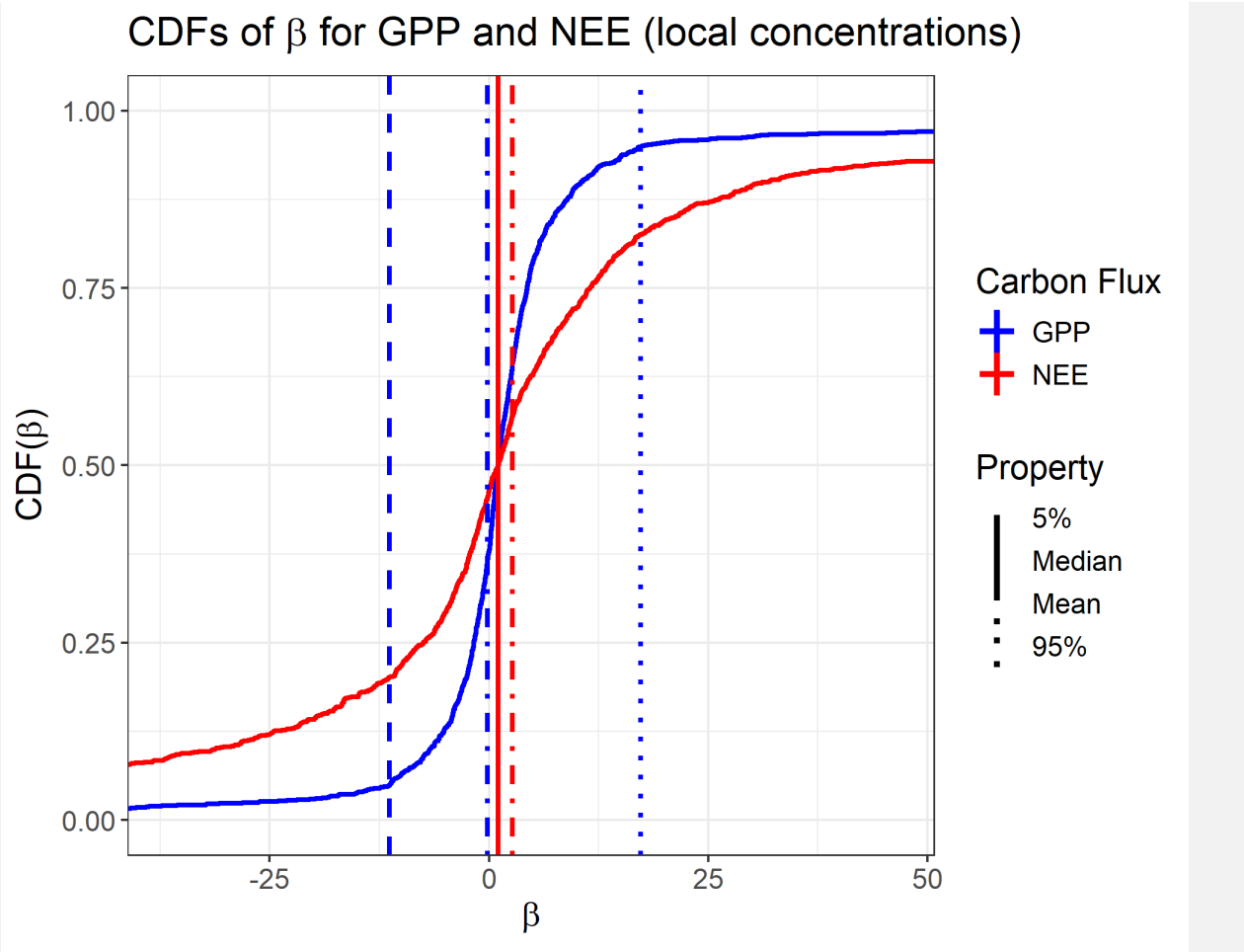

Figure 1: Distribution of the β values based on local concentration values, all sites taken together. β_{GPP} results in blue, β_{NEE} in red. The limits on the horizontal axis are given by the $[5\%, 95\%]$ interval for the broader distribution, i.e. β_{NEE}.

The medians of the two distributions are both positive and are closer to each other than the width of the solid vertical bar ($med(\beta_{GPP}) = 1.02$ vs. $med(\beta_{NEE}) = 1.07$). Mean values are $< \beta_{GPP} >= -0.18$ and $< \beta_{NEE} >= 2.67$.

Given the pace of CO_2 concentration globally, which is around $2\ ppm\ yr^{-1}$, local annual concentrations differing by less than $1\ ppm$ (say) over a period of several years point rather to a calibration issue of the IrGA. Nevertheless, we considered all combinations of flux and concentration values whenever present into account and obtained the values shown in Figure 1 as cumulative distribution, separated according to GPP and NEE. The NEE distribution is much broader than that of GPP, but both have significantly positive medians according to a Wilcoxon signed-rank test.

Using global CO_2 annual concentrations instead, the extreme outliers disappear, but the broader distribution of β_{NEE} remains; the respective distributions are not even significantly different according to Kolmogorov-Smirnov tests ($p_{GPP}(local|global) = 0.078$; $p_{NEE}(global|local) = 0.13$); the median for GPP and NEE are now different from each other and in particular, that of NEE is no longer significantly different from zero (Figure 2).

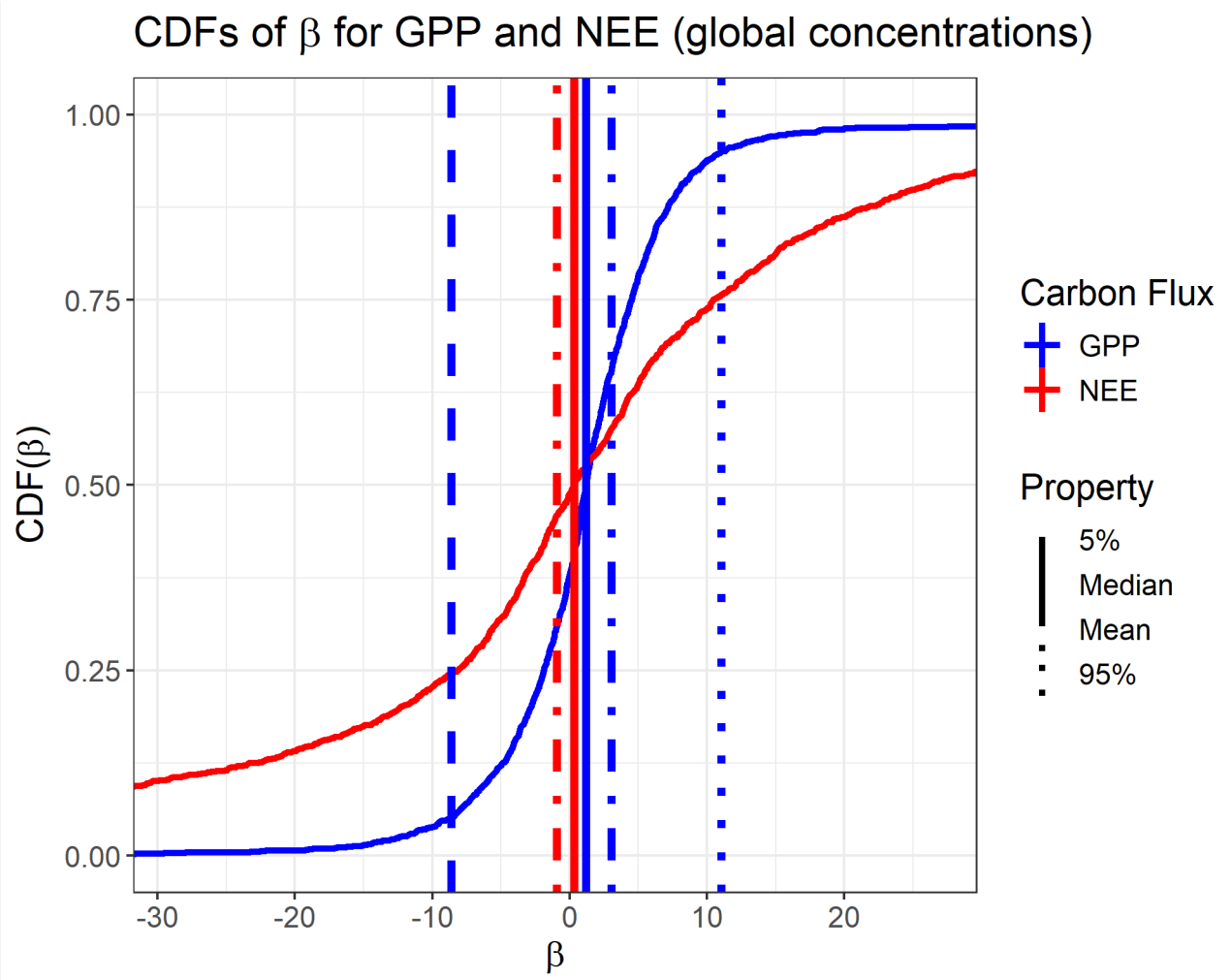

Figure 2: Same as Figure 1 but using global CO_2 concentrations. The two pairs of distributions ($\beta_{GPP}local|global$ and $\beta_{NEE}local|global$) are not significantly different.

However, the total number of β values obtained for the global concentrations is higher, since there are a couple of years where site-specific local annual concentrations were not available. Therefore, we continue the analysis with the β values based on *global* concentrations.

The dependence of the β estimates on the window time length is visible in Figure 3, where histograms where based only on β values with $|\beta| \leq 30$ which encompasses 98% of the β_{GPP} and 82% of the β_{NEE} values, respectively. The total counts are of course diminishing with larger window lengths since there are less pairs

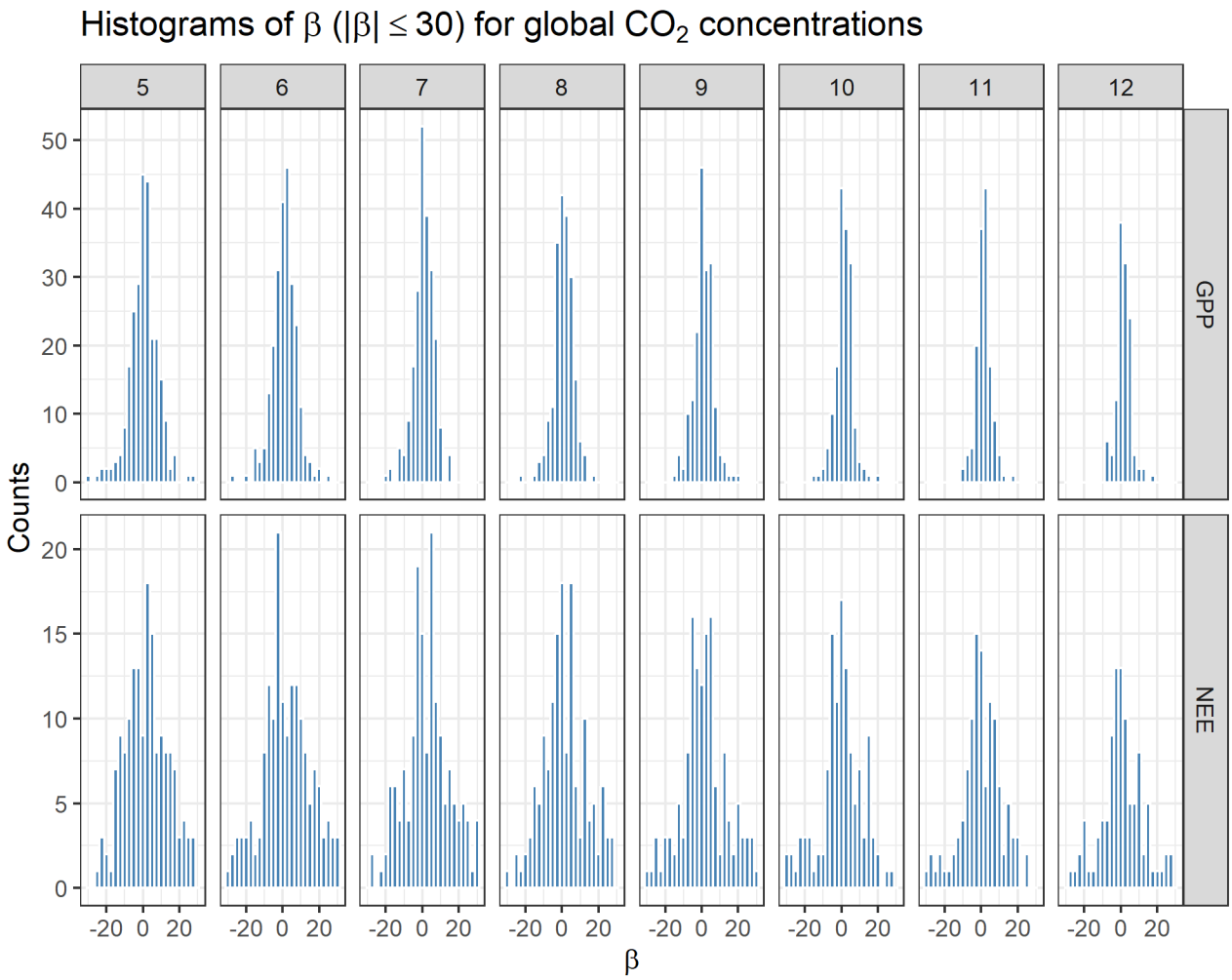

Figure 3: Histograms of the β values for global concentrations, depending on the time window length. This length is given at the top in years (from 5 to 12 years). Independent of that length, the distribution of β_{GPP} is sharper than that of β_{NEE}, but the distribution peak is very close to the bin containing zero. Note that the vertical scales are different between the upper and the lower panel.

with that temporal distance, but the histogram shape seems to be rather robust otherwise. This impression is confirmed by a rigorous comparison for all window lengths using the Kolmogorov-Smirnov test, as shown in Figure 4. There are only few significant differences, between rather short and rather long window lengths as expected. The robustness of the distributions and the need to consider rather long time spans to judge on the existence of a sink saturation effect let us choose the fixed window length of $\boldsymbol{\Delta T = 10}$ **years** for the regression analysis.

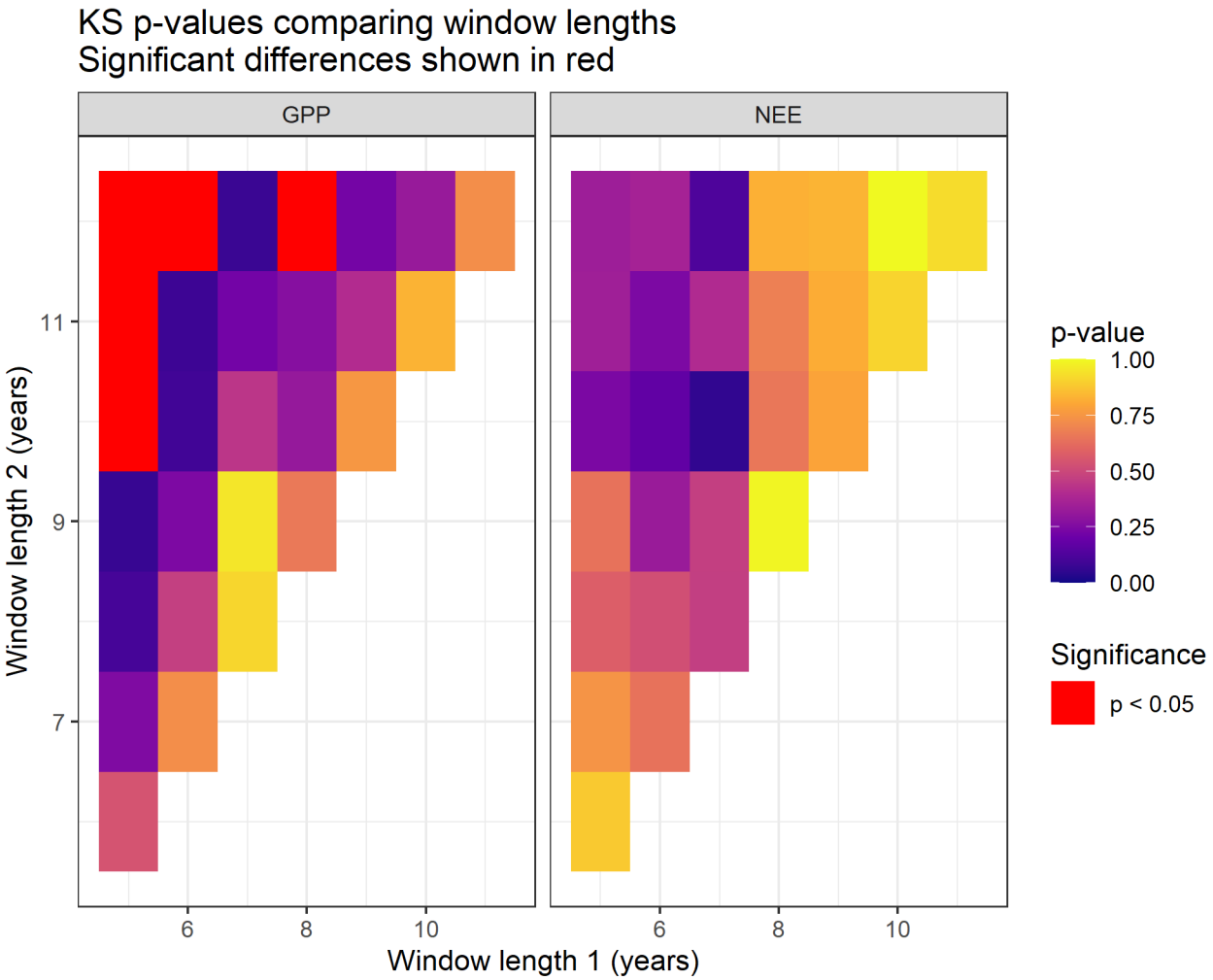

Figure 4: p values of the Kolmogorov-Smirnov tests. Comparisons which pass the significance test for the hypothesis "The two β distributions are different" with the threshold $p_{signif} = 0.05$ are shown in red.

Sign and significance for non-vanishing β slopes

At the fixed temporal separation of 10 years, there is a distribution of β slopes for any given station, determined by the length of the carbon flux record. Exceptional climate conditions like severe droughts may reduce GPP and the magnitude of NEE, rendering β negative despite strictly increasing annual CO_2 concentrations. As we are interested in the overall long-term behaviour, we test for the average value spectrum of β per site. Figure 5 shows box-and-whisker plots for both fluxes. It is apparent again that the β_{NEE} distributions are much less constrained compared to the β_{GPP} ones, and out of the only two mean values significantly different from zero, one is even negative. However, also the β_{GPP} mean values are mostly compatible with zero, and in a few cases even negative. This suggests that the forest ecosystems at the selected sites do not exhibit a strong or consistent positive response to increased atmospheric CO2 concentrations. That ecosystems benefit from additional CO_2 in the atmosphere is not convincingly supported by the flux tower records selected here. Some of the sites have so few observations at this window length that a calculation of the distribution shape is not even possible; they appear as single short lines in Figure 5.

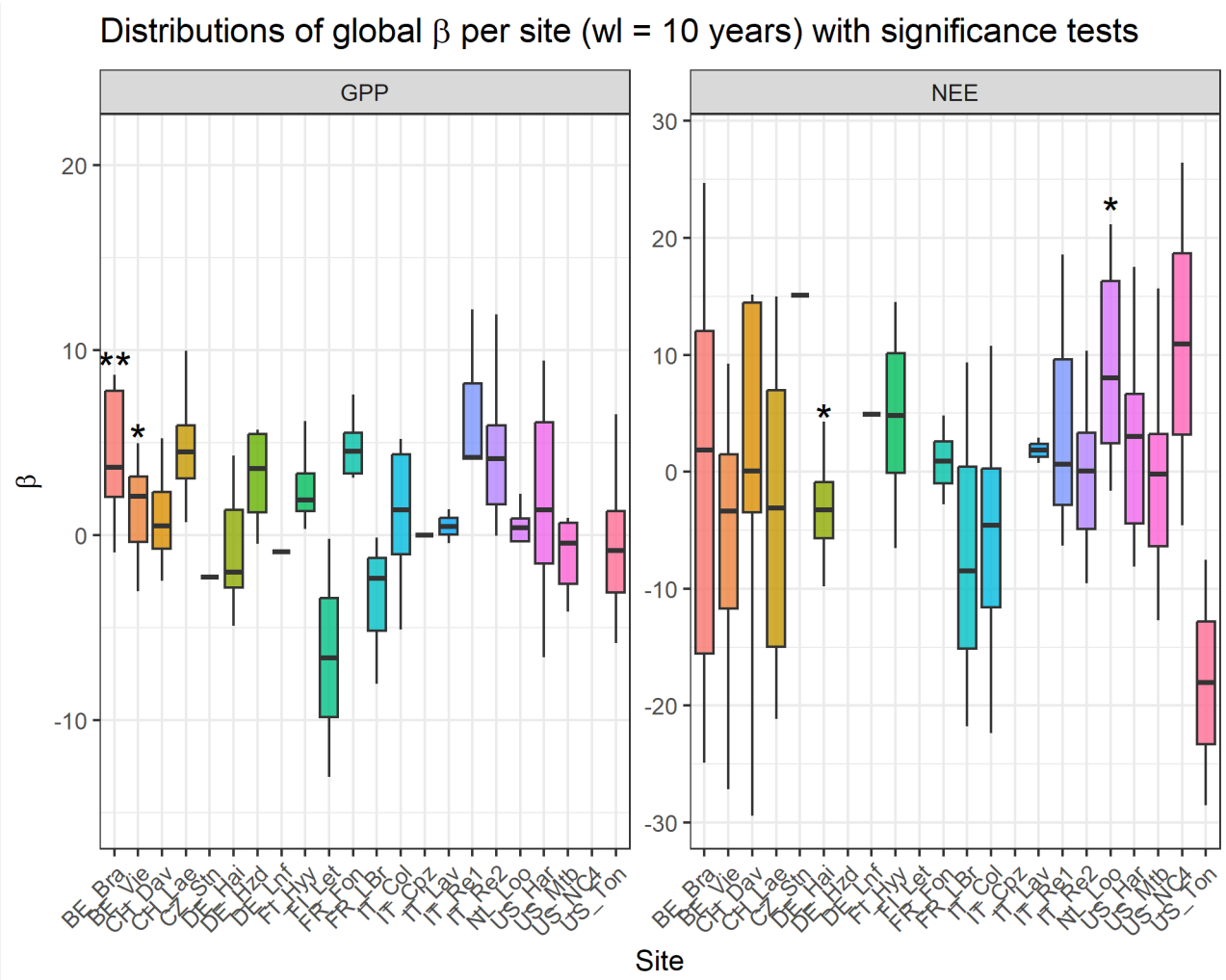

Figure 5: Box-and-whisker plot for the β values per site at fixed window length 10 years. Site acronyms as shown in Table 1. Significance levels for being non zero: * $p < 0.05$, ** $p < 0.01$.

However, the distributions do not reveal the temporal structure of the slopes. A trend analysis is necessary where feasible. We do this in the simplest manner imaginable – through least-squares linear regression.

Regression analysis for the β slopes

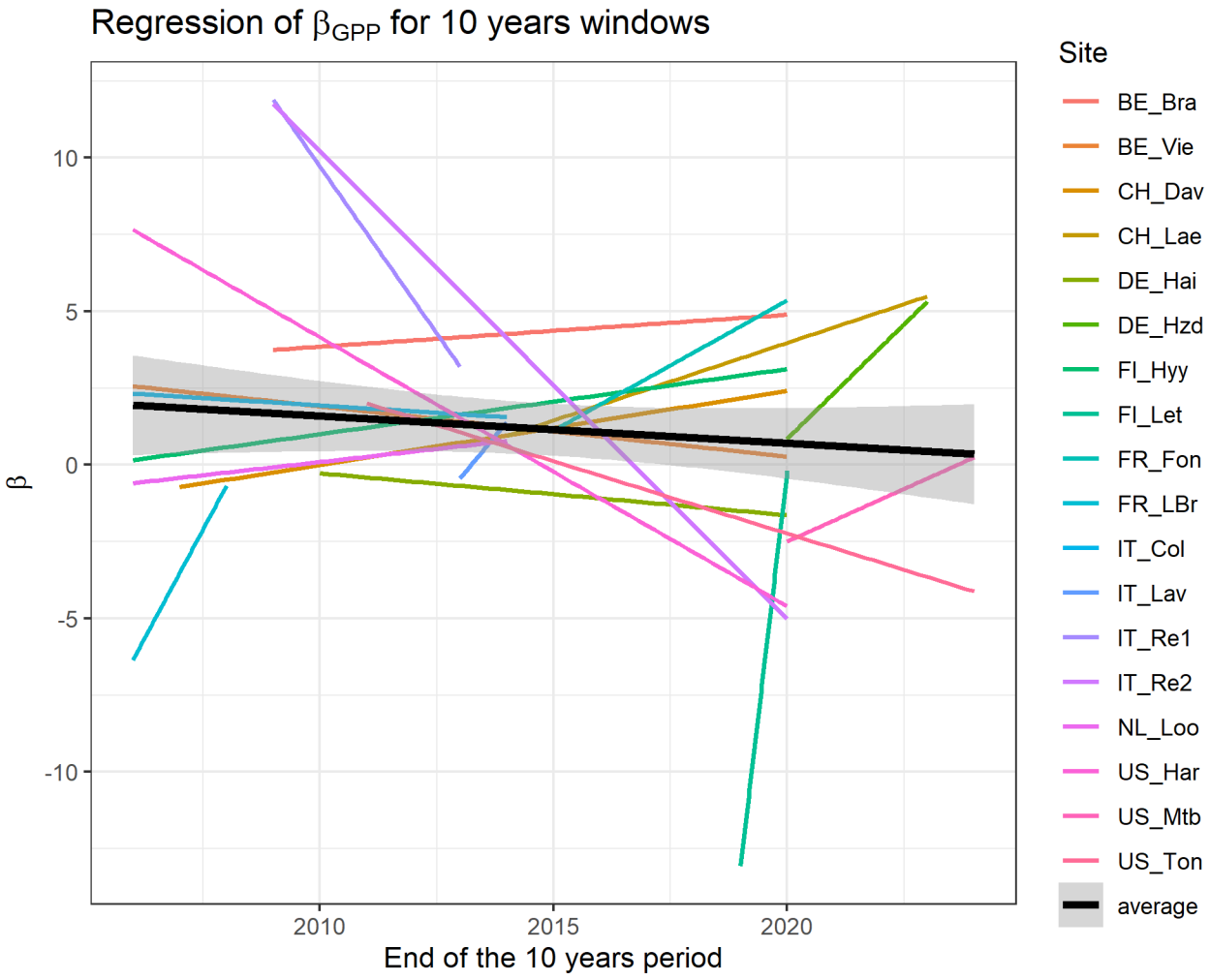

Figure 6: Regression lines for the β_{GPP} as obtained from each site, and for the average from all sites. For the latter, the 95% confidence interval is shown as grey area.

We calculated *slopes* of the β slopes, separately for each site and GPP and NEE, using the regression coefficient from a least-squares linear regression, ignoring missing values. Results for GPP are shown in Figures 6 and 7. None of the site data covers the whole period considered here (1996 – 2024) without gaps, therefore some of the lines are rather short, and the number of sites entering the average depends on the year.

The emerging pattern is diverse; there is no clear downward or upward trend. The average β_{GPP} has a negative slope and β_{NEE} a positive one; both of them are, however, not significant ($p_{\beta_{GPP}} = 0.24, p_{\beta_{NEE}} = 0.58$). The results are not conclusive: from the 18 sites where a slope calculation for β_{GPP} was possible., 9 show a positive trend, all of which not significant; the remaining 9 sites have a negative trend, only two of which are significant. For β_{NEE}, the same results hold, and the two sites with a significant negative trend are the same as for GPP. IT-Re2 and US-Har.

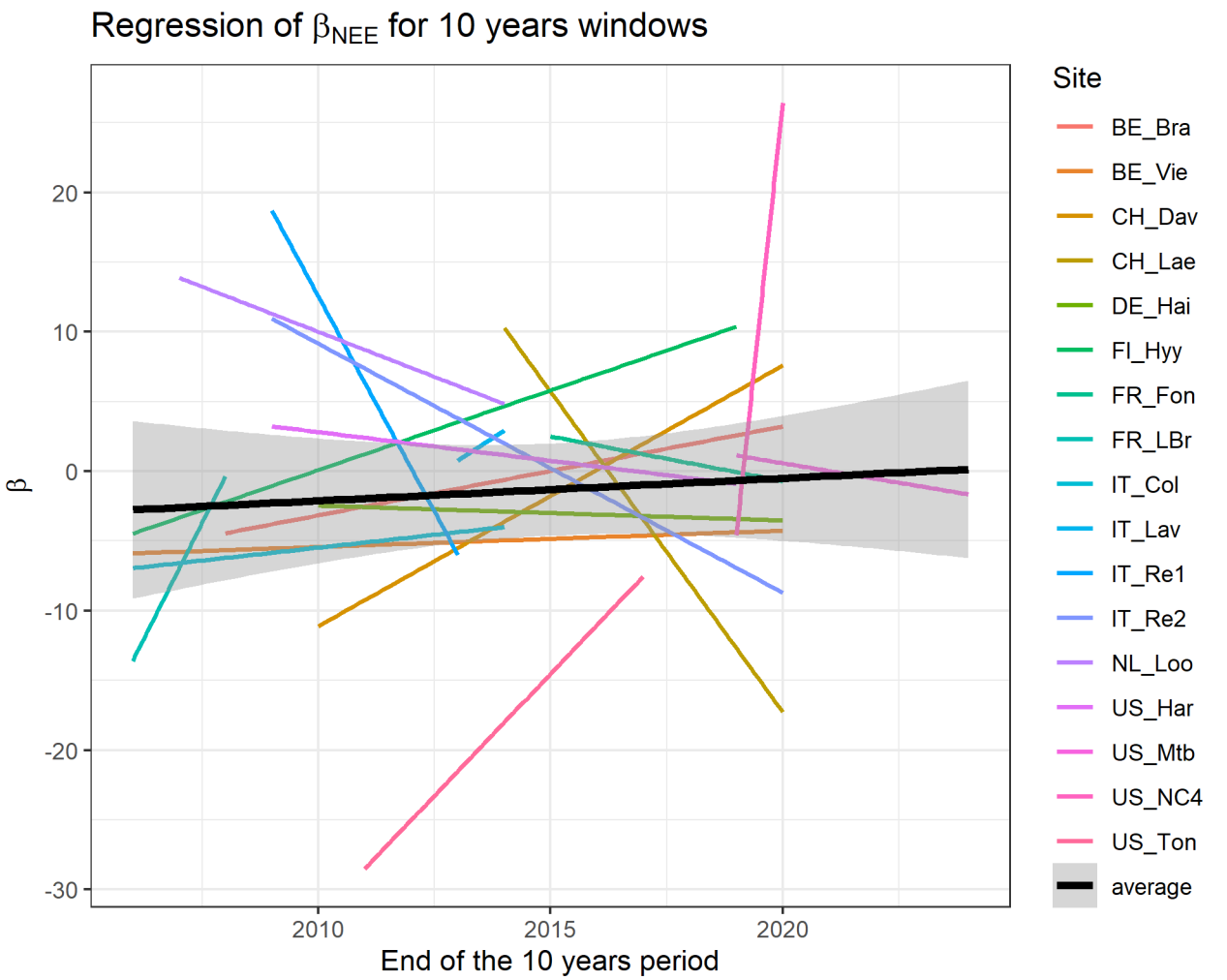

Figure 7: Same as Figure 6, but for β_{NEE}.

Example of a significant β slope: IT-Ren2

The connection between the annual CO_2 concentration and GPP for one of the sites, Renon in the Italian Alps, is visualized in Figure 8. The concentration axis could also be a time axis since on annual time scales, CO_2 concentrations are roughly linearly increasing during the last decades, with a slope averaging around $2\ ppm\ yr^{-1}$. The resulting β_{GPP} is based on moving 10-year time windows, the years covered by measurements being 1999 – 2020. It shows a clear significant negative slope, with β_{GPP} changing sign at higher concentrations, implying that for the last decade in the set, i.e. 2011-2020, the forest at Renon has a reduced GPP with increasing concentrations. There are numerous reasons for this behavior unrelated to increasing concentrations, such as disturbances, forest ageing, management operations, or responses to climate extremes. Investigations of these local conditions are outside the scope of this report but are likely to be important since the sites is one out of only two with a significant trend for β_{GPP}, i.e. the exception rather than the rule.

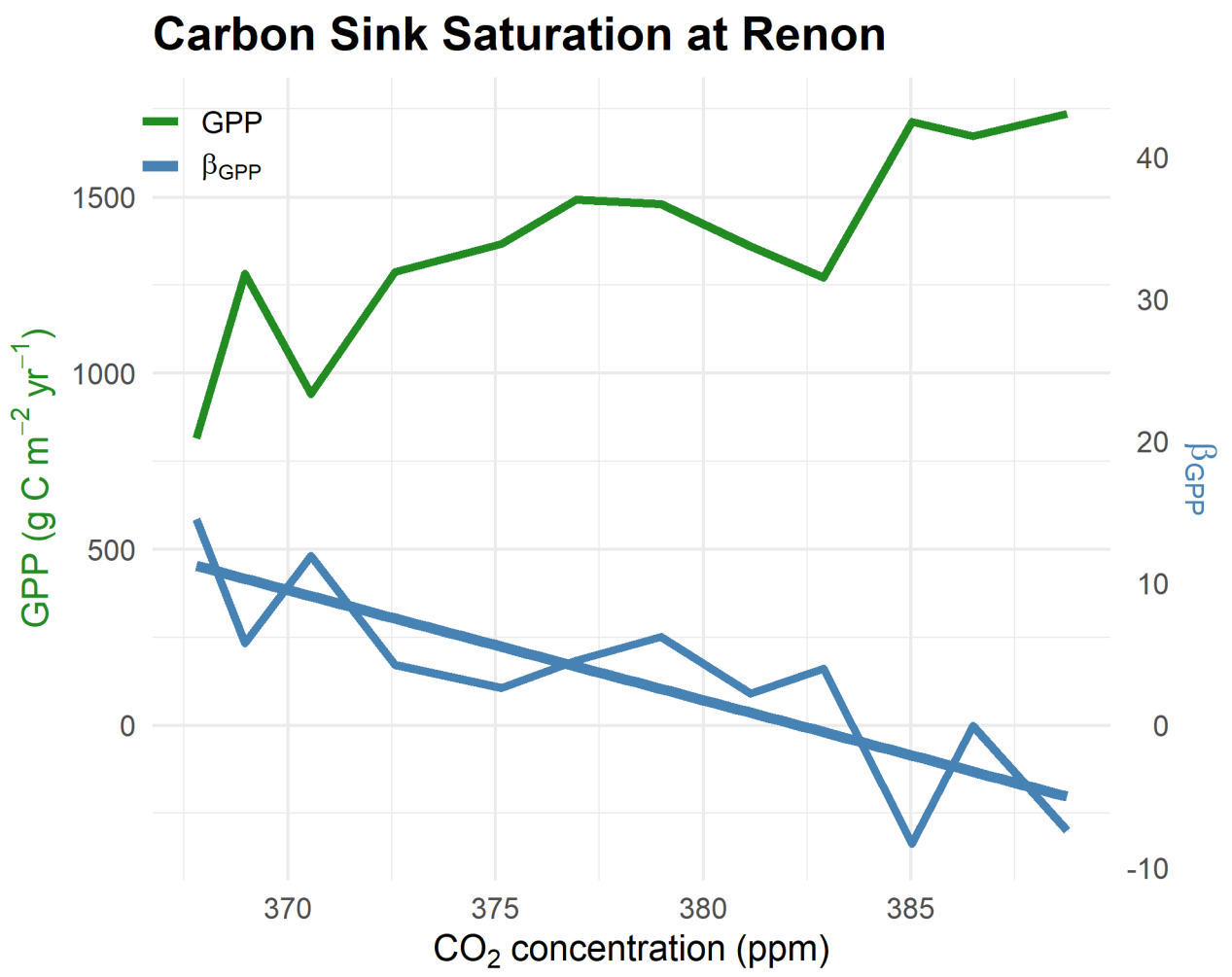

Figure 8: GPP and corresponding β_{GPP} for the site Renon in Italy as a function of global CO2 concentration. The trend for β_{GPP} is significant ($p = 7.9 \cdot 10^{-4}$).

Weakening of the CO_2 – GPP connection: a quantitative example

To put the trends in the β values into perspective, we convert them to the reduction in photosynthetic efficiency – the mass of carbon produced per time when increasing CO_2 concentration by a given amount – with units $g\ C\ m^{-2} yr^{-2} ppm^{-1}$. In order to do this, we need the time derivative of the ratios from eq. (3). Introducing for the ease of notification

$g(t) = \frac{GPP(t+\Delta t)}{GPP(t)}$ and $c(t) = \frac{CO_2(t+\Delta t)}{CO_2(t)}$, we have from eq. (3)

$\ln g(t) = \beta(t) \ln c(t)$ and thus for the time derivative

$$\frac{\frac{dg(t)}{dt}}{g(t)} = \frac{d\beta(t)}{dt} \log c(t) + \beta(t) \frac{\frac{dc(t)}{dt}}{c(t)} \quad (4)$$

The changes in GPP per CO_2 and time are then obtained by multiplying eq. (4) with $g(t)$ and then with $GPP(t)$, and dividing by $CO_2(t)$ to obtain the "saturation strength"

$$S_{sat} \overset{\text{def}}{=} \frac{dg(t)}{dt} \cdot \frac{GPP(t)}{CO_2(t)} = \left(\frac{d\beta(t)}{dt} \log c(t) + \beta(t) \frac{\frac{dc(t)}{dt}}{c(t)} \right) \frac{GPP(t+\Delta t)}{CO_2(t)} \quad (5)$$

The derivative $d\beta(t)/dt$ is simply the slope of β since we are doing a simple linear regression. With a reference time taken as the newest observations available, we calculate this "saturation strength" for GPP for the example above, the Renon site. The reference year is 2011 and $\Delta t = 10\,yrs$. Then $S_{sat} = -0.38\ g\ C\ m^{-2} yr^{-2} ppm^{-1}$. Considering the GPP *per ppm* of CO_2 at the site, this means that the *relative reduction of GPP increase per ppm* is around **9% per year**.

5. Conclusions

The site-level data for GPP and NEE, together with global concentrations of CO_2, do not provide compelling evidence for the presence of a carbon sink saturation. The regression analysis reveals that the slopes for the β values are compatible with zero in the majority of cases. The connection between CO_2 and GPP is, as expected, positive, i.e. forest ecosystems benefit from additional CO_2, but also here, there are some exceptions.

The analysis is constrained to the last approx. 25 years, as reliable records of Eddy Covariance-based flux measurements do not extend further back in time. This might be too short a period to reach firm conclusions, since the relative change in concentrations during this period amounted to around 15% only. Drought during the growing season, disturbances by extreme events, and reduced productivity due to ageing of the stands, are additional factors masking the potential saturation effect. The number of EC stations considered in this study is not very high (n=22), but it appears unlikely that taking into account further stations from other continents, mostly South America or Asia, would change the overall conclusion that site-level data are unable to confirm the hypothesis of an imminent carbon sink saturation for forests.

6. References

Friedlingstein, P. et al., 2025. Global Carbon Budget 2025. Earth Syst. Sci. Data Discuss., 2025: 1-139.

Korosuo, A. et al., 2023. The role of forests in the EU climate policy: are we on the right track? Carbon Balance and Management, 18(1): 15.

Nabuurs, G.-J. et al., 2013. First signs of carbon sink saturation in European forest biomass. Nature Clim. Change, 3(9): 792-796.

Nabuurs, G.-J., Schelhaas, M.-J., Mohren, G.f.M.J. and Field, C.B., 2003. Temporal evolution of the European forest sector carbon sink from 1950 to 1999. Global Change Biology, 9(2): 152-160.

Norby, R.J. and Zak, D.R., 2011. Ecological Lessons from Free-Air CO2 Enrichment (FACE) Experiments. Annual Review of Ecology, Evolution, and Systematics, 42(1): 181-203.

Randerson, J.T. et al., 2025. The weak land carbon sink hypothesis. Science Advances, 11(37): eadr5489.

Shi, H. et al., 2021. Saturation of Global Terrestrial Carbon Sink Under a High Warming Scenario. Global Biogeochemical Cycles, 35(10): e2020GB006800.

Walker, A.P. et al., 2021. Integrating the evidence for a terrestrial carbon sink caused by increasing atmospheric CO2. New Phytologist, 229(5): 2413-2445.

Wang, S. et al., 2020. Recent global decline of CO_2 fertilization effects on vegetation photosynthesis. Science, 370(6522): 1295-1300.

Project Partners

CLIMB-FOREST

Working closely with the forestry sector and policy makers, CLIMB-FOREST aims to ensure Europe's forests are resilient to the changing climate and support people and nature.

www.climbforest.eu
@ClimbForest

This project has received funding from the European Union's Horizon Europe research and innovation programme under grant agreement No 101059888